

FRACTIONAL CALCULUS IN POPULATION DYNAMICS

by

Ashlin Powell Harris

A Dissertation
Submitted in Partial Fulfilment
of the Requirements for the Degree of
Doctor of Computational Science

Middle Tennessee State University
December 2021

Dissertation Committee:
Dr. Abdul Khaliq, advisor
Dr. Wandi Ding
Dr. William Robertson
Dr. Zachariah Sinkala

DEDICATION

This dissertation is dedicated to Dr. Tibor Koritsanszky.

ACKNOWLEDGEMENTS

I would like to thank my doctoral advisor, Dr. Abdul Khaliq, for the guidance that I have received from him. I am also grateful for the assistance and feedback of my dissertation committee. Dr. Richard Magin was the first to suggest the implications of fractal biology to my research, and I owe him a cup of coffee. Finally, I would like to acknowledge Dr. Toheeb Biala for his integral role in every stage of this research.

ABSTRACT

*Mathematics is the art of giving the
same name to different things.*

HENRI POINCARÉ

Research in recent decades has incorporated fractional derivatives into partial differential equation models of natural phenomena. This generalisation to a non-integer order provides a way to describe anomalous diffusion within fractal spaces. However, most numerical methods developed for the integer order are not suited for efficient computation of these systems. In this work, we develop a method to numerically solve a multi-component and multi-dimensional space-fractional system. For space discretization, we apply a Fourier spectral method that is suited for multidimensional systems. Efficient approximation of time-stepping is accomplished with an exponential time differencing approach. We consider the convergence and stability of the methods and observe the effect of different fractional parameters. While the scope of this research is limited to the dynamics of biological systems, these same techniques may be applied to other disciplines.

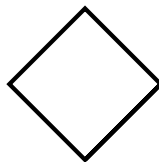


TABLE OF CONTENTS

List of Figures	vi
List of Tables	vii
List of Abbreviations	viii
1 Introduction	1
1.1 Population dynamics	1
1.2 Anomalous diffusion	2
1.3 Reaction-diffusion equations	3
2 Methods	5
2.1 Space discretization	5
2.1.1 Matrix transfer technique	5
2.1.2 Fourier spectral method	7
2.2 Time discretization	8
2.2.1 Backward Euler scheme	10
2.2.2 Crank-Nicolson scheme	10
3 Numerical Experiments	11
3.1 One-dimensional system	11
3.2 Two-dimensional system	15
4 Conclusion	18
Bibliography	20
Appendix	21

LIST OF FIGURES

3.1	One-dimensional system, BE and CN schemes	12
3.2	Solution profiles and leading edges	13
3.3	Absolute error as a function of time step size	13
3.4	Absolute error as a function of CPU time	13
3.5	Two-dimensional system, ETD-CN scheme	16

LIST OF TABLES

3.1	Slopes of initial spread	14
3.2	Rates of convergence	15

LIST OF ABBREVIATIONS

- BE - backward Euler
- CN - Crank-Nicolson
- CPU - central processing unit
- ETD - exponential time differencing
- MTT - matrix transfer technique
- ODE - ordinary differential equation
- PDE - partial differential equation
- RD - reaction-diffusion (Or is it reproduction-dispersal ...?)

CHAPTER 1: INTRODUCTION

*It is not birth, marriage, or death, but
gastrulation which is truly the most
important time in your life.*

LEWIS WOLPERT

In the study of anomalous diffusion, Baeumer, Kovács, and Meerschaert have described fractional-order reproduction dispersal equations, which can be solved efficiently by the Fourier spectral method of Bueno-Orovio, Kay, and Burrage.^[1,2] We build upon the analysis of Marcus Garvie and generalise his predator-prey system to the non-integer order, adapting the aforementioned method in conjunction with the exponential time differencing approach of Ilic, Liu, Turner, and Anh.^[3,4] During the course of our research, Hala Ashi has established the feasibility and benefit of this generalisation, providing us with invaluable guidance for our own work.^[5]

This chapter describes the use of fractional models in population dynamics. Within this Introduction, Section 1.1 describes the underlying biological systems that motivate our research. Anomalous diffusion is described in Section 1.2, and Section 1.3 introduces the class of reaction-diffusion equations. Afterwards, mathematical descriptions of our numerical techniques are given in Chapter 2, with results in Chapter 3 and closing remarks in Chapter 4.

1.1 POPULATION DYNAMICS

Density (or abundance) of a biological species is the relative representation of a species in a region and is typically defined as the number of individuals found per sample. Incidence, the mere presence or absence of a species, is more easily measured than density but is less informative for the study of invasiveness, which is the rate at which a species may establish and spread. Invasions are influenced by abiotic and stochastic factors, but our focus is on intrinsic measures of invasiveness, such as the reproduction number of pathogens.

Species generally exhibit low density wherever they are incident, with high density in relatively few regions. Though sometimes attributed to temporal variation of population size, this trend holds true at various spatial scales and may be considered a fundamental biological phenomenon, at least in ecology.^[6]

There is no consensus on the distinction between “invasive” and “non-invasive” for non-native species, but high density has served as an operational definition. The potential to invade other regions has been observed in relatively few species; most introduced species do not become invasive.^[7] On average, a species with higher incidence exhibits higher density than a species with lower incidence. Of course, a species must spread outside of its native region to be considered invasive. Assuming that the species is not being driven out of its native region, this constitutes an increase in incidence. Invasive species are therefore expected to exhibit higher density.^[6]

Invasiveness can be distinguished from impact, which refers to the effect that an invasive species has on native species. The density of a species is related to its environmental impact, but certain species may have a disproportionately large effect. These include keystone species, whose presence at low numbers in a particular region may help increase overall biodiversity. In contrast, the presence of a non-native species may reduce species diversity. Of course, the interactions between two species often are more nuanced and complex than this.^[8]

Even very simple deterministic models may exhibit complex dynamics, with the possibility of chaotic behaviour.^[9] Garvie discusses chaos as an ecological phenomenon and observes the influence of varying parameters on the level of chaos in his mathematical model. For certain initial conditions, these systems develop spiral patterns which evolve into irregular patches, which conforms to what is observed in nature.^[3]

1.2 ANOMALOUS DIFFUSION

Diffusion, the gradient-driven net movement of a substance, is a topic of study in all natural sciences. Mathematical models of diffusion include partial differential equations and random walks. Recently, attention has been given to anomalous diffusion, which features a stable non-linear relationship between mean squared displacement and time. This can be modelled in terms of fractional-order differential equations and Lévy flights. In the context of physics and chemistry, anomalous diffusion is often described as a fractional-order movement within ordinary space, whereas biologists tend to describe anomalous diffusion in terms of a fractional-order dimension of the time or space; that is, entities exhibit classical diffusion over a fractal space.^[10] Anomalous diffusion is divided into subdiffusion, which describes the slow diffusion of substances within crowded or self-similar media, and superdiffusion, which describes active transport and some species invasions.

Anomalous diffusion is observed in complex polymer networks and materials packed with varying sizes of pores or obstacles. Within these media, particles travel in a hierarchy of different time

scales, so the overall mean-square displacement is modelled in terms of a power-law.^[1] With sufficient complexity across scales (that is, if the space becomes no simpler when we zoom in), the space can be modelled as a fractal. Anomalous diffusion due to barriers occurs at all time scales (even at thermal equilibrium) if the concentration of obstructions exceeds the percolation threshold.^[11]

Biological anomalous diffusion may occur across widely diverse scales in simultaneity, and the same models that govern biochemical reactions have been used to describe interactions between cells, organisms, and populations. Interestingly, the eukaryotic cell interior provides instances of anomalous diffusion of molecules in one-dimensional (transport along microfilaments), two-dimensional (diffusion across plasma membranes), and three-dimensional space (diffusion within crowded cytoplasm).^[12,13] Anomalous diffusion might also describe the dispersal of cells within an organism (by migration or metastasis), pathogens within a population, or ecological species within an environment. As an example at this scale, Baeumer, Kovács, and Meerschaert have proposed the use of fractional-in-space models to capture realistic spreading behaviour of invading species.^[1]

1.3 REACTION-DIFFUSION EQUATIONS

Reaction-diffusion equations have been used to describe the movement and interaction of species in various contexts, especially chemistry and biology. In 1952, Alan Turing published a reaction-diffusion model for morphogenesis in order to explain biological features such as self-organisation, stability, and symmetries in terms of a simple chemical system.^[14] Morphogenic models describe many topics within developmental biology, including animal markings, limb bud formation, and cell fate determination.

The original predator-prey model was first developed independently by Alfred James Lotka (to describe autocatalytic chemical reactions) and by Vito Volterra (to describe population dynamics).^[15,16] Since then, reaction-diffusion models have been used extensively in the study of ecological predator-prey interactions and have been rephrased as reproduction-dispersal models in this context. These systems are influenced primarily by the functional response; that is, the rate at which an individual predator consumes prey. The diffusion terms of nonlinear reaction diffusion problems tend to be stiff, which constrains the step size of any fully explicit numerical solution.^[5]

Equation 1.1 shows the classical reaction-diffusion equation

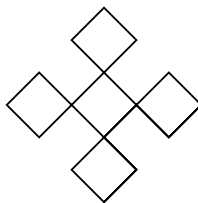
$$\frac{\partial u}{\partial t} = \mathbf{D} \frac{\partial^2 u}{\partial x^2} + \mathbf{f}(u), \quad (1.1)$$

by which the density u is governed across space x and time t . In this formulation for systems, \mathbf{D} is a diagonal matrix of diffusion components and $\mathbf{f}(u)$ is the vector of reaction terms. For most biologically informative systems, density is strictly positive and exhibits periodic oscillations. Interference to these systems can permanently alter their trajectory, perhaps with unintended consequence. For instance, adding predators at some stages of the cycle can result in a greater prey population, an unfortunate outcome of some historical pest reduction programs.

Partial differential equations classically have been limited to integer derivatives, though the idea of a generalisation to a non-integer order fractional is nearly as old (it was proposed by Leibniz); their use in scientific models is much more recent. The classical reaction-diffusion equation (Equation 1.1), once generalised to include a real number derivative, becomes

$$\frac{\partial u}{\partial t} = \mathbf{D} \frac{\partial^\alpha u}{\partial x^\alpha} + \mathbf{f}(u). \quad (1.2)$$

The value of α constrained to $1 < \alpha \leq 2$, where the special case $\alpha = 2$ yields the classical reaction-diffusion equation again. This generalised model can be used to describe biologically relevant anomalous diffusion.



CHAPTER 2: METHODS

A good numerical method, like a good spouse, is reliable, stable, efficient.

A. Q. M. KHALIQ

Natural systems can have several components which react and diffuse across multiple spatial dimensions. These behaviours may be defined in terms of partial differential equations whose general solutions are unknown, though they might be approximated to arbitrary precision by numerical methods. Relevant methods for numerically solving space fractional PDEs are described by Aceto and Novati.^[17] Our objective is to develop methods for multi-component and multi-dimensional biological systems.

In Section 2.1, we describe two methods for space discretization: the Matrix Transfer Technique (Subsection 2.1.1) and a Fourier spectral method (Subsection 2.1.2). Section 2.2 explains the exponential time differencing approach for time discretization, and for this we give two numerical schemes: the fully implicit backward Euler (Subsection 2.2.1), and the semi-implicit Crank-Nicolson (Subsection 2.2.2).^[18]

2.1 SPACE DISCRETIZATION

The Matrix Transfer Technique was developed originally by Ilić, Liu, Turner, and Anh.^[4] It is highly efficient for one-dimensional systems, and we adapt it as described in Subsection 2.1.1 for our own analysis. The Fourier spectral method scales well for systems with higher dimension, and we show our adaptation in Subsection 2.1.2.

2.1.1 Matrix transfer technique

Consider the fractional reaction-diffusion equation (Equation 1.2). To discretise the system with endpoints a and b , Let $x_i = ih$ for $i = 0, \dots, N$, where $h = (b - a)/N$ is the space step size. Once the spatial derivative has been discretised, we have a system whose elements are of the form

$$\frac{\partial u(x, t)}{\partial t} = -D_i \left(-\frac{\partial^2}{\partial x^2} \right)^{\frac{\alpha}{2}} u(x, t) + f(u), \quad (2.1)$$

where D_i is the diffusion coefficient, δ_x^2 is the second-order central difference operator, and $u_i(t) = u(x_i, t)$ for $i = 1, \dots, N-1$. With the following definitions,

$$\begin{aligned}\mathbf{U}(t) &:= [u_1(t), u_2(t), \dots, u_{N-2}(t), u_{N-1}(t)]^T, \\ \mathbf{F}(\mathbf{U}) &:= [f(x_1, t, u), f(x_2, t, u), \dots, f(x_{N-1}, t, u)]^T,\end{aligned}\tag{2.2}$$

we can use a finite difference approximation to rewrite all the elements of Equation 2.1 in matrix form as

$$\frac{d\mathbf{U}(t)}{dt} = -\mathbf{D} \frac{\mathbf{A}}{h^2} \mathbf{U}(t) + \mathbf{F}(\mathbf{U}), \quad t = 0, 1, 2, \dots,\tag{2.3}$$

where \mathbf{A} is the simple tridiagonal matrix of order $(N-1) \times (N-1)$ given by

$$\mathbf{A} = \begin{pmatrix} 2 & -1 & & & \\ -1 & \ddots & \ddots & & \\ & \ddots & \ddots & -1 & \\ & & -1 & 2 & \end{pmatrix}_{(N-1, N-1)}.\tag{2.4}$$

The matrix \mathbf{A} in turn can be diagonalised as $\mathbf{A} = \mathbf{T}\mathbf{\Lambda}\mathbf{T}^{-1}$, where \mathbf{T} is an $(N-1) \times (N-1)$ matrix such that

$$\mathbf{T}_{i,j} = \sin\left(\frac{ij\pi}{N}\right),\tag{2.5}$$

and $\mathbf{\Lambda}$ is an $(N-1) \times (N-1)$ diagonal matrix defined as

$$\mathbf{\Lambda}_{i,j} = \begin{cases} 4 \sin^2\left(\frac{i\pi}{2l}\right) & \text{for } i = j, \\ 0 & \text{elsewhere.} \end{cases}\tag{2.6}$$

Let $\frac{\mathbf{A}}{h^2} = \left(-\frac{\partial^2}{\partial x^2} \mathbf{U}\right)$, which is the matrix representation of the Laplace operator with homogeneous boundary conditions. Given that

$$\left(-\frac{\partial^2}{\partial x^2} \mathbf{U}\right)^{\frac{\alpha}{2}-1} = \left(\frac{\mathbf{A}}{h^2}\right)^{\frac{\alpha}{2}-1},\tag{2.7}$$

the matrix system of Equation 2.3 is rewritten as

$$\frac{d\mathbf{U}(t)}{dt} = -\kappa \left(\frac{\mathbf{A}}{h^2}\right)^{\frac{\alpha}{2}-1} \left(\frac{\mathbf{A}}{h^2}\right) \mathbf{U}(t) + \mathbf{F}(\mathbf{U})\tag{2.8}$$

to finally be converted to a system of ODEs in the form

$$\frac{d\mathbf{U}(t)}{dt} = -\frac{\kappa}{h^\alpha} (\mathbf{T}\mathbf{\Lambda}^{\frac{\alpha}{2}}\mathbf{T}^{-1}) \mathbf{U}(t) + \mathbf{F}(\mathbf{U}), \quad t = 0, 1, 2, \dots \quad (2.9)$$

2.1.2 Fourier spectral method

For the space discretization, we adapt the spectral methods developed by Bueno-Orovio, Kay, and Burrage.^[2] We begin with the reaction-diffusion system for the vector of species densities $\mathbf{u} = [u_1, u_2, \dots, u_M]^T$ governed by

$$\frac{\partial u_i}{\partial t} = -D_i (-\Delta)^{\alpha/2} u_i + f_i(\mathbf{u}), \quad (2.10)$$

where D_i is the diffusion coefficient of the i^{th} species u_i and $f_i(\mathbf{u})$ is its reaction term. Suppose that the Laplacian $(-\Delta)$ has a complete set of orthonormal eigenfunctions ϕ_n , $\phi_{n,m}$, or $\phi_{n,m,l}$, depending on its dimension, corresponding to the eigenvalues λ_n , $\lambda_{n,m}$, or $\lambda_{n,m,l}$, respectively, on a bounded region Ω . That is, for each of $n, m, l = 0, 1, 2, \dots$ in Ω ,

$$\begin{aligned} (-\Delta)\phi_n &= \lambda_n \phi_n, & (d=1), \\ (-\Delta)\phi_{n,m} &= \lambda_{n,m} \phi_{n,m}, & (d=2), \\ (-\Delta)\phi_{n,m,l} &= \lambda_{n,m,l} \phi_{n,m,l}, & (d=3), \end{aligned} \quad (2.11)$$

and $\mathcal{B}(\phi) = 0$ on $\partial\Omega$, where $\mathcal{B}(\phi)$ are the homogeneous Dirichlet or homogeneous Neumann boundary conditions. Let

$$\begin{aligned} f_1 &= \sum_{n=0}^{\infty} c_n \phi_n & \text{such that } \sum_{n=0}^{\infty} |c_n|^2 |\lambda_n|^\alpha < \infty, & (d=1), \\ f_2 &= \sum_{n=0}^{\infty} \sum_{m=0}^{\infty} c_{n,m} \phi_{n,m} & \text{such that } \sum_{n=0}^{\infty} \sum_{m=0}^{\infty} |c_{n,m}|^2 |\lambda_{n,m}|^\alpha < \infty, & (d=2), \\ f_3 &= \sum_{n=0}^{\infty} \sum_{m=0}^{\infty} \sum_{l=0}^{\infty} c_{n,m,l} \phi_{n,m,l} & \text{such that } \sum_{n=0}^{\infty} \sum_{m=0}^{\infty} \sum_{l=0}^{\infty} |c_{n,m,l}|^2 |\lambda_{n,m,l}|^\alpha < \infty, & (d=3). \end{aligned} \quad (2.12)$$

Then, $(-\Delta)^{\frac{\alpha}{2}}$ is defined by

$$\begin{aligned} (-\Delta)^{\frac{\alpha}{2}} f_1 &= \sum_{n=0}^{\infty} c_n \lambda_n^{\frac{\alpha}{2}} \phi_n, & (d=1), \\ (-\Delta)^{\frac{\alpha}{2}} f_2 &= \sum_{n=0}^{\infty} \sum_{m=0}^{\infty} c_{n,m} \lambda_{n,m}^{\frac{\alpha}{2}} \phi_{n,m}, & (d=2), \\ (-\Delta)^{\frac{\alpha}{2}} f_3 &= \sum_{n=0}^{\infty} \sum_{m=0}^{\infty} \sum_{l=0}^{\infty} c_{n,m,l} \lambda_{n,m,l}^{\frac{\alpha}{2}} \phi_{n,m,l}, & (d=3). \end{aligned} \quad (2.13)$$

For the homogeneous Dirichlet (solution value) boundary conditions with $d \in \{1, 2, 3\}$, $\Omega = (a, b)^d$, and $\mathbf{x} \in \Omega$, we have

$$\begin{aligned}\lambda_{1,\dots,d} &= \sum_{n=1}^d \left(\frac{(n+1)\pi}{b-a} \right)^2, \\ \phi_{1,\dots,d} &= \left(\sqrt{\frac{2}{b-a}} \right)^d \prod_{n=1}^d \sin \left(\frac{(n+1)\pi(x_n - a)}{b-a} \right).\end{aligned}\tag{2.14}$$

Alternatively, the homogeneous Neumann (derivative value) boundary conditions are given by

$$\begin{aligned}\lambda_{1,\dots,d} &= \sum_{n=1}^d \left(\frac{n\pi}{b-a} \right)^2, \\ \phi_{1,\dots,d} &= \left(\sqrt{\frac{2}{b-a}} \right)^d \prod_{n=1}^d \cos \left(\frac{n\pi(x_n - a)}{b-a} \right).\end{aligned}\tag{2.15}$$

By applying a Fourier transform and the definition of the fractional Laplacian (Equation 2.13) to Equation 2.10, we obtain (for $d = 1$)

$$\frac{\partial \hat{u}_{ij}}{\partial t} = -D_i \lambda_j^{\alpha/2} \hat{u}_{ij} + \hat{f}_{ij}(\hat{\mathbf{u}}),\tag{2.16}$$

where \hat{u}_{ij} is the j^{th} Fourier coefficients of the i^{th} species and \hat{f}_{ij} is its associated reaction term. Due to the orthogonality of the basis functions, each of the Fourier coefficients evolve independently of the others. For the grid points in space $j = 1, 2, \dots, N$ and step size h , the corresponding homogeneous Dirichlet boundary conditions are

$$\lambda_j = \frac{j\pi}{b-a}, \quad x_j = a + jh + \frac{h}{2}, \quad h = \frac{(b-a)}{N+1},\tag{2.17}$$

and the homogeneous Neumann boundary conditions are given by

$$\lambda_j = \frac{(j-1)\pi}{b-a}, \quad x_j = a + (j-1)h + \frac{h}{2}, \quad h = \frac{(b-a)}{N}.\tag{2.18}$$

We compute the coefficients \hat{u}_i and the inverse reconstruction of u in space using coefficient algorithms (discrete sine or cosine transforms and their inverses) based on the specified homogeneous boundary conditions.^[2]

2.2 TIME DISCRETIZATION

Non-linear biological models motivate the use of exponential time differencing methods.^[5] The methods in this section are based on the work of Kleefeld, Khaliq, and Wade.^[19] Several ETD

schemes can be recovered from Equation 2.21 by different approximations to the exponential function and the integral term. In particular, we discuss the ETD Backward Euler Scheme (ETD-BE) and the ETD Crank-Nicolson scheme (ETD-CN).

Consider the Fourier transform of $u(x)$ into $\hat{u}(k)$ on \mathbb{R} , and its inverse

$$\begin{aligned}\hat{u}(k) &= \frac{1}{2\pi} \int_{-\infty}^{\infty} u(x) e^{-ikx} dx, k \in \mathbb{R}, \\ \hat{u}(x) &= \int_{-\infty}^{\infty} \hat{u}(k) e^{ikx} dk, x \in \mathbb{R},\end{aligned}\tag{2.19}$$

with physical variable x and Fourier wavenumber k . At first, we rewrite Equation 2.16 as

$$\frac{\partial \hat{U}_i}{\partial t} = -D_i \Lambda^{\alpha/2} \hat{U}_i + \hat{F}_i(\hat{\mathbf{U}}),\tag{2.20}$$

where \hat{U} and \hat{F} are the vectors of Fourier coefficients of the i^{th} species and the respective reaction terms with physical variable x and Fourier wavenumber k . Let $t_k = k\tau$ for $k = 0, \dots, N$, where $\tau = T/N$ is the time step size and $\hat{U}(t_k) = \hat{U}^k$. Here, the exact solution of Equation 2.20 at time t_{k+1} can be written as

$$\hat{U}_i(t_{k+1}) = e^{-\tau\Lambda^{\frac{\alpha}{2}}} \hat{U}_i(t_k) + \tau \int_0^1 e^{-\tau\Lambda^{\frac{\alpha}{2}}(1-s)} \hat{F}_i(\hat{\mathbf{U}}(t_k + s\tau)) ds.\tag{2.21}$$

Equation 2.21 serves as the basis for exponential time differencing schemes which are obtained from different approximations to the matrix exponential function and the nonlinear reaction terms. Suppose $\hat{F}_i(\hat{\mathbf{U}})$ from Equation 2.21 is approximated by an average over end points in the interval $[t_k, t_{k+1}]$. That is,

$$\begin{aligned}\hat{F}_i(\hat{\mathbf{U}}) &\approx \hat{F}_i(\hat{\mathbf{U}}^k) + (t - t_k) \frac{\hat{F}_i(\hat{b}^k) - \hat{F}_i(\hat{\mathbf{U}}^k)}{\tau}, \quad t \in [t_k, t_{k+1}], \\ \hat{b}^k &= e^{-\tau\Lambda^{\frac{\alpha}{2}}} \hat{U}_i^k + \Lambda^{-\frac{\alpha}{2}} \left(I - e^{-\tau\Lambda^{\frac{\alpha}{2}}} \right) \hat{F}_i(\hat{\mathbf{U}}^k).\end{aligned}\tag{2.22}$$

The integral in Equation 2.21 then becomes

$$\hat{U}^{k+1} \approx e^{-\tau\Lambda^{\frac{\alpha}{2}}} \hat{U}^k + \tau e^{-\tau\Lambda^{\frac{\alpha}{2}}} \int_0^1 e^{\tau\Lambda^{\frac{\alpha}{2}} s} \left(\hat{F}_i(\hat{\mathbf{U}}^k) + \tau \frac{\hat{F}_i(\hat{b}^k) - \hat{F}_i(\hat{\mathbf{U}}^k)}{\tau} \right) ds,\tag{2.23}$$

which simplifies to

$$\hat{U}_i^{k+1} \approx \hat{b}^k + \frac{1}{\tau} \Lambda^{-\alpha} \left(e^{-\tau\Lambda^{\frac{\alpha}{2}}} - I + \tau\Lambda^{\frac{\alpha}{2}} \right) \left[\hat{F}_i(\hat{b}^k) - \hat{F}_i(\hat{\mathbf{U}}^k) \right].\tag{2.24}$$

2.2.1 Backward Euler scheme

The simplest approximation to the Equation 2.21 is obtained by defining the reaction term $\mathbf{F}(\mathbf{U})$ by $\mathbf{F}(U_k) := \mathbf{F}_k$, which yields the approximation

$$\mathbf{U}_{k+1} \approx e^{-\tau A^{\frac{\alpha}{2}}} \mathbf{U}_k + A^{-\frac{\alpha}{2}} \left(\mathbf{I} - e^{-\tau A^{\frac{\alpha}{2}}} \right) \mathbf{F}_k \quad (2.25)$$

Approximating the exponential function in Equation 2.25 by the [0,1]-Padé approximant yields the backward Euler ETD scheme (ETD-BE):

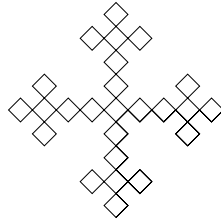
$$\mathbf{U}_{k+1} \approx \left(I + \tau A^{\frac{\alpha}{2}} \right)^{-1} (\mathbf{U}_k + \tau \mathbf{F}_k). \quad (2.26)$$

2.2.2 Crank-Nicolson scheme

Alternatively, if the exponential matrix in Equation 2.24 is replaced by the [1,1]-Padé approximant, the Crank-Nicolson ETD scheme (ETD-CN) is obtained, after some simplification, as

$$\begin{aligned} \hat{V}_i^{k+1} &= \hat{\mathbf{a}}^k + \tau \left(2I + \tau \Lambda^{\frac{\alpha}{2}} \right)^{-1} \left[\hat{F}_i(\hat{\mathbf{a}}^k) - \hat{F}_i(\hat{\mathbf{V}}^k) \right] \approx \hat{U}_i^{k+1}, \\ \hat{\mathbf{a}}^k &= \left(4 \left(2I + \tau \Lambda^{\frac{\alpha}{2}} \right)^{-1} - I \right) \hat{V}_i^k + 2\tau \left(2I + \tau \Lambda^{\frac{\alpha}{2}} \right)^{-1} \hat{F}_i(\hat{\mathbf{V}}^k). \end{aligned} \quad (2.27)$$

The convergence and unconditional stability of Equation 2.27 follows from Khaliq, Biala, Alzahrani, and Furati with some slight modification.^[20]



CHAPTER 3: NUMERICAL EXPERIMENTS

*Clouds are not spheres, mountains are
not cones, coastlines are not circles,
and bark is not smooth, nor does
lightning travel in a straight line.*

BENOIT MANDELBROT

This chapter describes our implementation of the exponential time differencing methods of Kleefeld, Khaliq, and Wade for numerically solving a fractional reaction-diffusion equation.^[19] We show the effect of different fractional parameters on growth models, with special attention to the tails of distribution profiles. Section 3.1 contains our analysis of a predator-prey system with fractional diffusion in one-dimensional space. In Section 3.2, we analyse the extension for multiple dimensions for a two-dimensional predator-prey model with two separate Holling-type interaction terms.

3.1 ONE-DIMENSIONAL SYSTEM

For space discretization, we use the Matrix Transfer Technique, developed by Ilic, Liu, Turner, and Anh, which is highly efficient for 1-dimensional systems.^[4] The results of our simulations are visualised in Figure 3.1 for both the backward Euler and Crank-Nicolson schemes. We simulate the results of Baeumer, Kovács, and Meerschaert for additional values of α and analyse the spreading behaviour in Figure 3.2 and Table 3.1.^[1] The two schemes themselves are analysed and compared in Figure 3.3 and Figure 3.4 and summarised in Table 3.2.

Figure 3.1 shows surface plots of the reaction-diffusion equation with exponential time differencing for different values of α using two numerical schemes (backward Euler and Crank-Nicolson). The system contains a single species U which is initially present around the origin. Over time, the species reproduces and disperses through the system. In this illustrative example, a rather large step size $\tau = 1.0$ is used, so differences between the backward Euler and Crank-Nicolson methods are apparent. At $\alpha = 2$, the system behaves under classical diffusion, and as this value becomes lower, the fractional effect of anomalous diffusion becomes more pronounced.

Figure 3.1: One-dimensional system, BE and CN schemes

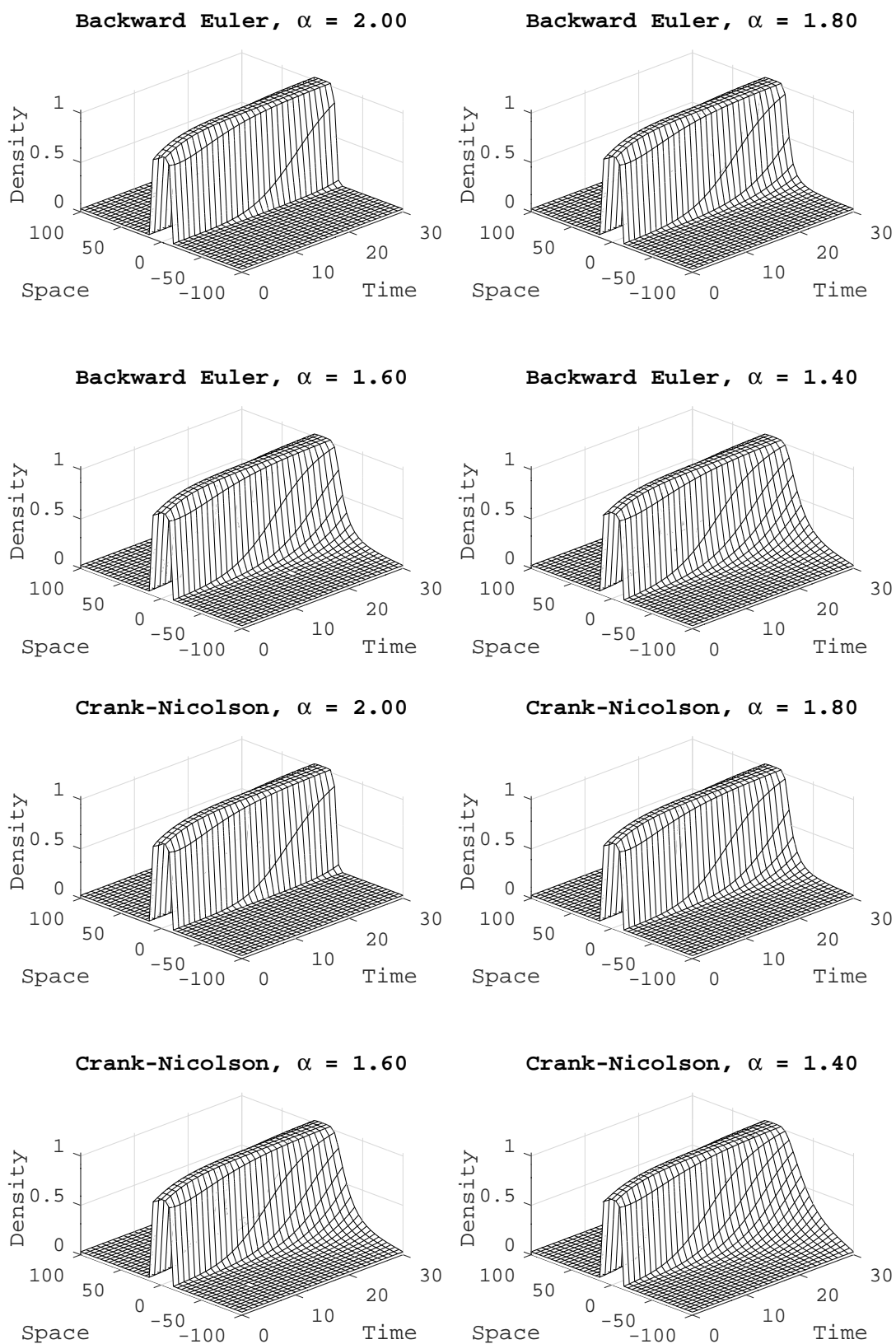


Figure 3.2: Solution profiles and leading edges

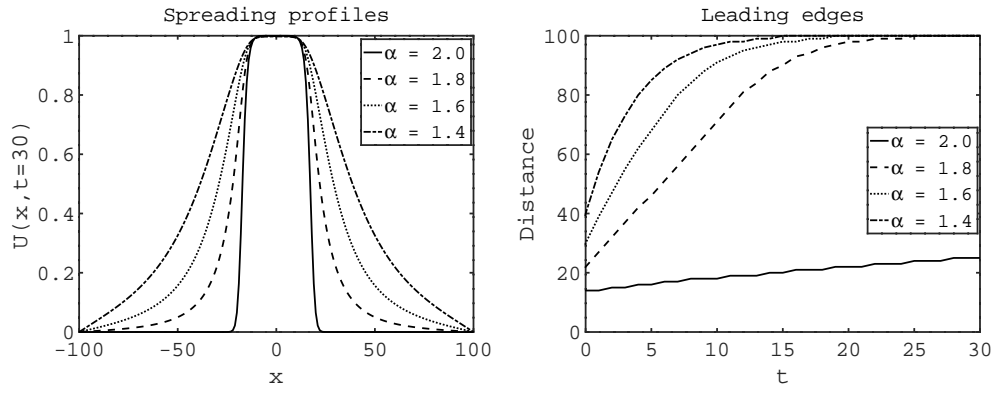


Figure 3.3: Absolute error as a function of time step size

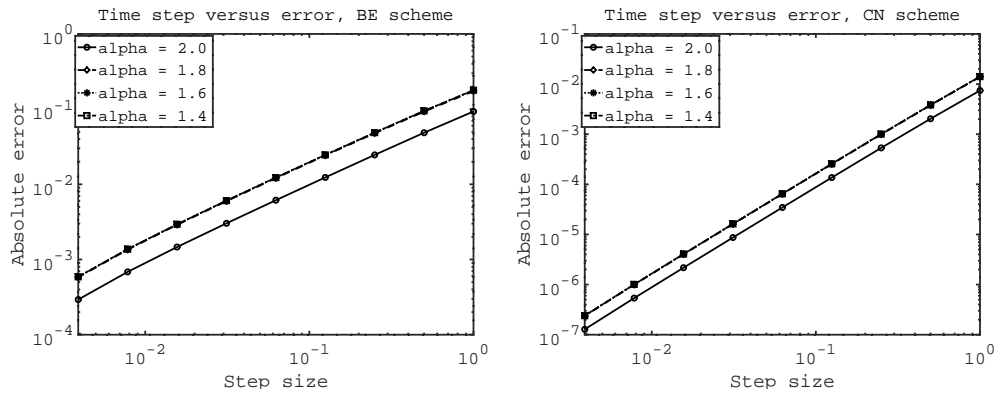
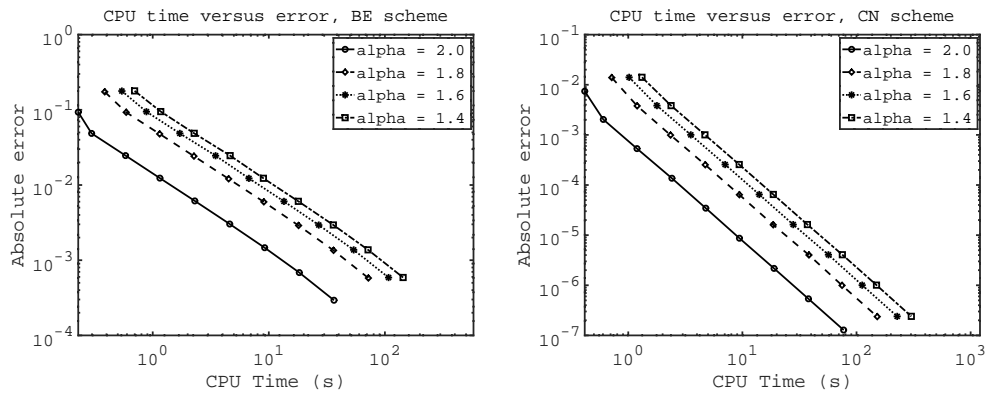


Figure 3.4: Absolute error as a function of CPU time



This difference is examined in Figure 3.2, which shows the spreading behaviour at each value of α under the Crank-Nicolson scheme. Similar results (not shown) may be obtained from the backward Euler scheme, but as discussed below, both schemes converge towards the true values for a sufficiently small time step. Along with Baeumer, Kovács, and Meerschaert, we observe at the final time (shown on the left graph) a steep spreading profile in the classical case but a fat-tailed distribution in the fractional case.^[1] This corresponds with more rapid dispersal under anomalous diffusion, as seen in the graph on the right, where for each time step, the greatest distance at which there is some incidence of the species is plotted. Here can be seen a significant difference between the integer and non-integer order diffusion, where the spread is linear with respect to time in the classical case only. This is analogous to the effect observed in mean squared displacement, which is linear-in-time only for integer-order diffusion.

The effect is given further attention in Table 3.1. Here, for additional values of α not represented graphically, we compare the initial rate of incidence spreading as described above. The slopes are calculated on in the region from time $t = 0$ to $t = 5$, where spreading is approximately linear. After this interval, a boundary effect dominates the rate of spread in the fractional case.

In Figure 3.3, we examine error as a function of time step. Since the exact solutions of these equations are unknown, for the error calculations, a numerical solution obtained from with a very small time step is used as the analytical solution. We observed no significant difference in accuracy at different values of $\alpha < 2$, though sparse solvers might potentially outperform these for values very close to 2. In our implementation, the Crank-Nicolson method outperformed the backward Euler for any size of time step. As shown in Table 3.2, rates of convergence calculated from this data correspond with the theoretical predictions, regardless of the α value; the backward Euler method is order 1, and the Crank-Nicolson method has second-order convergence

Table 3.1: Slopes of initial spread

α	Slope
2.0	0.9
1.9	3.5
1.8	5.2
1.7	6.6
1.6	8.4
1.5	10.2
1.4	12.2

Table 3.2: Rates of convergence

α	Backward-Euler	Crank-Nicolson
2.0	1.031	1.980
1.8	1.022	1.982
1.6	1.023	1.982
1.4	1.024	1.982

in time. However, there exists a space of step sizes for which the semi-implicit Crank-Nicolson exhibits spurious oscillations to which the fully implicit backward Euler method is immune.^[21]

We also consider error as a function of CPU time spent (Figure 3.4). Again, we see that calculations are more efficient for classical diffusion under either scheme. This is expected, as operations on the diagonal matrix of the non-fractional case are much more efficient than on the dense matrix associated with the nonlocality of the fractional case. However, here we do observe differences in performance based on the order of diffusion; as α decreases, computational time increases. Error sizes are smaller in the classical case, but when the case $\alpha = 2$ is excluded, we see significant no difference in error size between α values. As before, the Crank-Nicolson method outperforms the backward Euler.

3.2 TWO-DIMENSIONAL SYSTEM

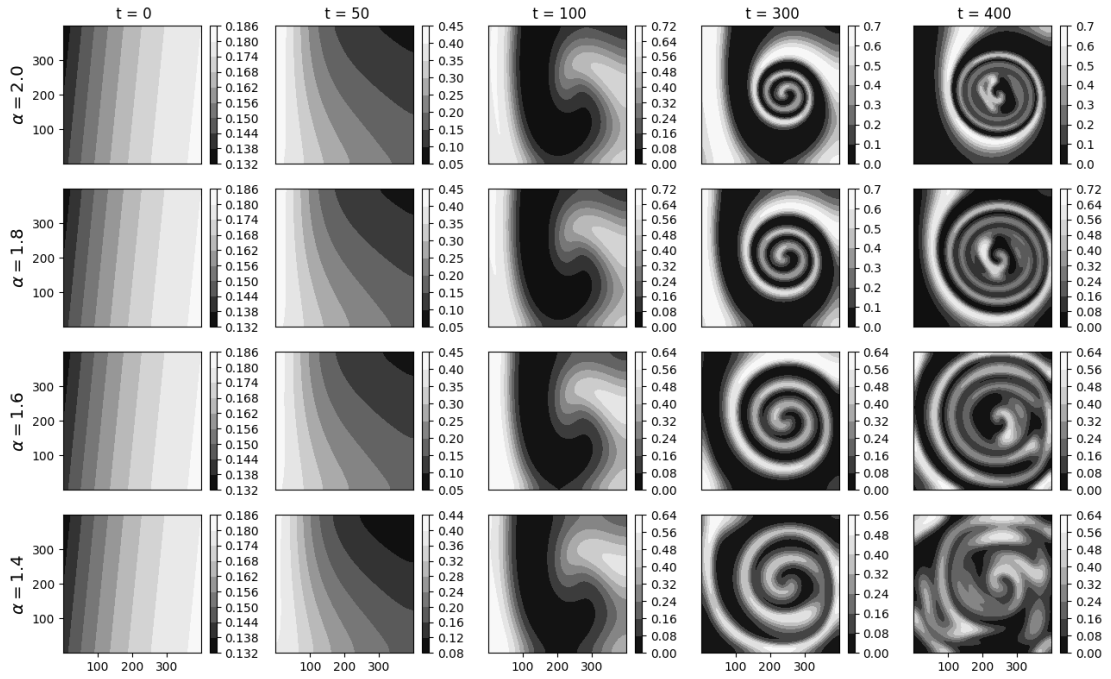
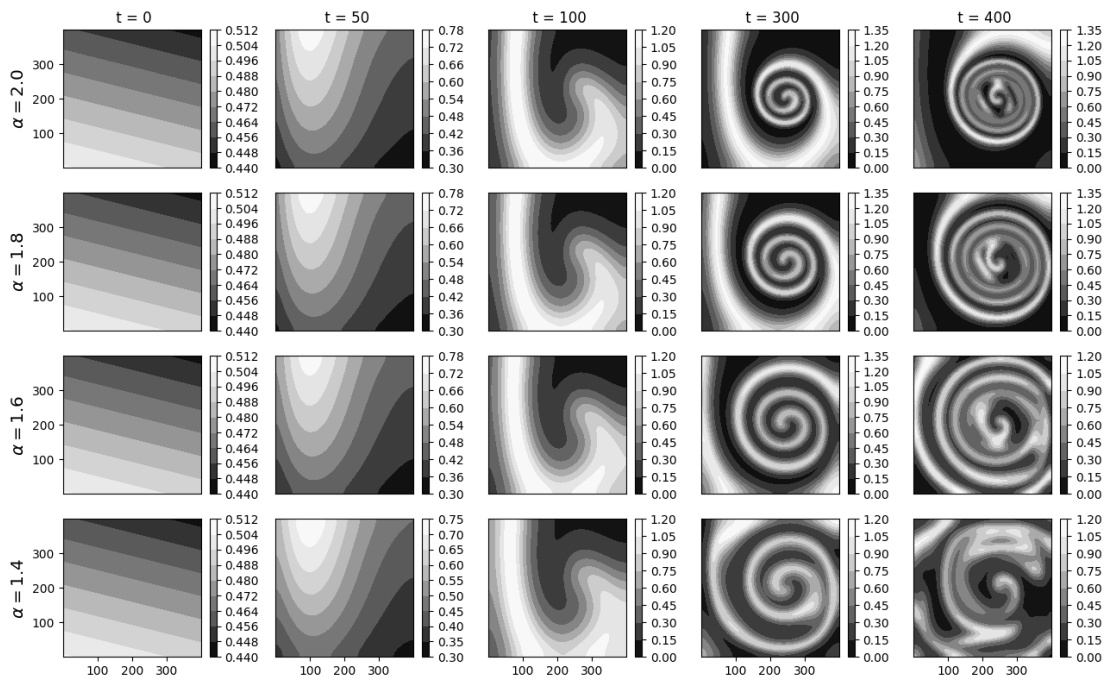
For space discretization, we use a Fourier spectral method which scales efficiently for multiple dimensions. For time discretization, we use the exponential time differencing approach with a Crank-Nicolson scheme. The results of the 2-dimensional simulation are shown in Figure 3.5.

The following model is Garvie's non-dimensional formulation of a predator-prey system that has been generalised for a fractional derivative:^[3]

$$\begin{aligned}\frac{\partial u}{\partial t} &= \Delta^{\alpha/2}u + u(1 - u) - vh(au), \\ \frac{\partial v}{\partial t} &= \delta\Delta^{\alpha/2}v + bv h(au) - cv.\end{aligned}\tag{3.1}$$

The population density of the prey species is denoted by u , and the predator species population density is denoted by v . Each population density is considered over time t and vector position \vec{x} . The Laplace operator is designated as Δ . The functional response h , defined as the rate of prey consumption per predator relative to the maximum, increases strictly on $[0, \infty]$ and satisfies $h(0) = 0$ and $\lim_{x \rightarrow \infty} h(x) = 1$. All remaining variables a , b , c and δ are parameters of the predator-prey system and strictly positive. This deterministic model does not include an abiotic

Figure 3.5: Two-dimensional system, ETD-CN scheme

(a) Density of U (b) Density of V

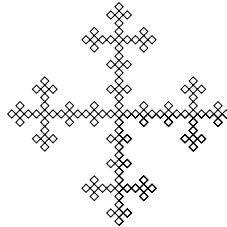
component and does not account for stochastic factors. We use the type II functional response proposed by Crawford Holling:^[22]

$$h(au) = \frac{au}{1 + au}. \quad (3.2)$$

With the proposed methods, we evaluate Equation 3.1 with the parameters $a = \frac{1}{0.4}$, $b = 2.0$, $\gamma = 0.6$, and $\delta = 1.0$. The initial conditions are given by

$$\begin{aligned} U_{i,j}^0 &= \frac{6}{35} - 2 \times 10^{-7}(x_i - 0.1y_j - 225)(x_i - 0.1y_j - 675), \\ V_{i,j}^0 &= \frac{116}{245} - 3 \times 10^{-5}(x_i - 450) - 1.2 \times 10^{-4}(y_j - 150). \end{aligned} \quad (3.3)$$

The results for various alpha values are shown in Figure 3.5. We observe that complex, semi-stable patterns emerge from a simple gradient initial condition. As the value of α becomes lower, spreading behaviour becomes wider, which is characteristic for fractional-order diffusion.^[1] This faster spreading means that wave fronts will approach the boundaries sooner, which disrupts the spiral pattern that emerges. So, we observe the ecologically relevant dynamics described by Garvie, by which the system develops a spiral pattern which is taken over by chaotic patches, depending on the model parameters.^[3] Additionally, we find that the order of diffusion can influence the system evolution, with chaos arising sooner in the fractional case.



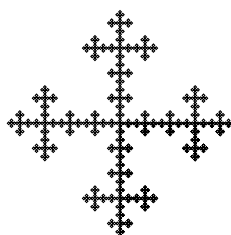
CHAPTER 4: CONCLUSION

Science is a differential equation.

Religion is a boundary condition.

ALAN TURING

Fractional reaction-diffusion models are suitable for the description of anomalous diffusion, especially in the context of biological species moving and interacting within fractal landscapes. The solution profiles of fractional reaction-diffusion equations have thicker tails than their integer-order counterparts, which can better describe many biological phenomena. The order of the derivative influences the appearance of chaotic behaviour in deterministic models of biological systems, perhaps providing an indication of the invasiveness of a biological species within its environment. Finally, the numerical methods we have adapted and described are suitable for numerically solving these models.



BIBLIOGRAPHY

- [1] B. Baeumer, M. Kovács, and M. M. Meerschaert, “Fractional reproduction-dispersal equations and heavy tail dispersal kernels,” *Bulletin of Mathematical Biology*, vol. 69, no. 7, pp. 2281–2297, 2007.
- [2] A. Bueno-Orovio, D. Kay, and K. Burrage, “Fourier spectral methods for fractional-in-space reaction-diffusion equations,” *BIT Numerical Mathematics*, vol. 54, no. 4, pp. 937–954, 2014.
- [3] M. R. Garvie, “Finite-difference schemes for reaction–diffusion equations modeling predator–prey interactions in MATLAB,” *Bulletin of Mathematical Biology*, vol. 69, no. 3, pp. 931–956, 2007.
- [4] M. Ilic, F. Liu, I. Turner, and V. Anh, “Numerical approximation of a fractional-in-space diffusion equation (II) – with nonhomogeneous boundary conditions,” *Fractional Calculus and Applied Analysis*, vol. 9, no. 4, pp. 333–349, 2006.
- [5] H. A. Ashi, “Solving stiff reaction-diffusion equations using exponential time differences methods,” *American Journal of Computational Mathematics*, vol. 8, no. 01, p. 55, 2018.
- [6] G. J. Hansen, M. J. Vander Zanden, M. J. Blum, M. K. Clayton, E. F. Hain, J. Hauxwell, M. Izzo, M. S. Kornis, P. B. McIntyre, A. Mikulyuk, E. Nilsson, J. D. Olden, M. Papeş, and S. Sharma, “Commonly rare and rarely common: comparing population abundance of invasive and native aquatic species,” *PLoS One*, vol. 8, no. 10, p. e77415, 2013.
- [7] M. Williamson and A. Fitter, “The varying success of invaders,” *Ecology*, vol. 77, no. 6, pp. 1661–1666, 1996.
- [8] M. L. Rosenzweig and R. H. MacArthur, “Graphical representation and stability conditions of predator-prey interactions,” *The American Naturalist*, vol. 97, no. 895, pp. 209–223, 1963.
- [9] R. M. May, “Simple mathematical models with very complicated dynamics,” *Nature*, vol. 261, no. 5560, pp. 459–467, 1976.
- [10] A. Johnson, B. Milne, and J. Wiens, “Diffusion in fractal landscapes: simulations and experimental studies of tenebrionid beetle movements,” *Ecology*, vol. 73, no. 6, pp. 1968–1983, 1992.

- [11] M. J. Saxton, “A biological interpretation of transient anomalous subdiffusion. I. Qualitative model,” *Biophysical Journal*, vol. 92, no. 4, pp. 1178–1191, 2007.
- [12] D. Krapf, “Mechanisms underlying anomalous diffusion in the plasma membrane,” *Current Topics in Membranes*, vol. 75, pp. 167–207, 2015.
- [13] B. M. Regner, D. Vučinić, C. Domnisoru, T. M. Bartol, M. W. Hetzer, D. M. Tartakovsky, and T. J. Sejnowski, “Anomalous diffusion of single particles in cytoplasm,” *Biophysical Journal*, vol. 104, no. 8, pp. 1652–1660, 2013.
- [14] A. M. Turing, “The chemical basis of morphogenesis,” *Bulletin of Mathematical Biology*, vol. 52, no. 1, pp. 153–197, 1990.
- [15] A. J. Lotka, “Contribution to the theory of periodic reactions,” *The Journal of Physical Chemistry*, vol. 14, no. 3, pp. 271–274, 1910.
- [16] V. Volterra, “Variations and fluctuations of the number of individuals in animal species living together,” *ICES Journal of Marine Science*, vol. 3, no. 1, pp. 3–51, 1928.
- [17] L. Aceto and P. Novati, “Rational approximation to the fractional Laplacian operator in reaction-diffusion problems,” *SIAM Journal on Scientific Computing*, vol. 39, no. 1, pp. A214–A228, 2017.
- [18] J. Crank and P. Nicolson, “A practical method for numerical evaluation of solutions of partial differential equations of the heat-conduction type,” in *Mathematical Proceedings of the Cambridge Philosophical Society*, vol. 43, pp. 50–67, Cambridge University Press, 1947.
- [19] B. Kleefeld, A. Khaliq, and B. Wade, “An ETD Crank-Nicolson method for reaction-diffusion systems,” *Numerical Methods for Partial Differential Equations*, vol. 28, no. 4, pp. 1309–1335, 2011.
- [20] A. Khaliq, T. Biala, S. Alzahrani, and K. M. Furati, “Linearly implicit predictor–corrector methods for space-fractional reaction–diffusion equations with non-smooth initial data,” *Computers & Mathematics with Applications*, vol. 75, no. 8, pp. 2629–2657, 2018.
- [21] J. D. Lawson and J. L. Morris, “The extrapolation of first order methods for parabolic partial differential equations. I,” *SIAM Journal on Numerical Analysis*, vol. 15, no. 6, pp. 1212–1224, 1978.
- [22] C. S. Holling, “The functional response of predators to prey density and its role in mimicry and population regulation,” *The Memoirs of the Entomological Society of Canada*, vol. 97, no. S45, pp. 5–60, 1965.

APPENDIX

*It seems surprising that so simple a
relation has not (to my knowledge)
been recognised before.*

GEORGE R. PRICE

This document was typeset in \LaTeX ^[1], with citation management in `natbib`^[2]. The mistakes herein are entirely my own; they are my only novel contribution to science. An iteration of the Vicsek fractal, shown at the end of each chapter, was drawn using the `lindenmayersystems` package of TikZ^[3]. Numerical simulations were implemented and results were plotted in GNU Octave^[4], though Figures 3.5 and 3.6 were plotted in Python 3^[5]. I have never heard of MATLAB. Most of the epigraphs are well known, at least in some circle. The quote from my advisor in Chapter 2 was inspired by that of another speaker, now forgotten. I have paraphrased the quote above from Price’s “Selection and covariance” (1970).

This manuscript must not be uploaded to ProQuest.

- [1] M. Goossens, F. Mittelbach, and A. Samarin, *The LaTeX companion*, vol. 1. Addison-Wesley Reading, 1994.
- [2] P. W. Daly, “Natural sciences citations and references,” 1999.
- [3] T. Tantau, “The TikZ and PGF packages,” *Manual for Version 2.10*, 2012.
- [4] J. W. Eaton, D. Bateman, S. Hauberg, and R. Wehbring, *GNU Octave version 4.4.0 manual: a high-level interactive language for numerical computations*, 2018.
- [5] G. Van Rossum and F. L. Drake, *Python 3 Reference Manual*. Scotts Valley, CA: CreateSpace, 2009.

